Thermal Characteristics of Selected EV and HEV Batteries

Ahmad A. Pesaran and Matthew Keyser
National Renewable Energy Laboratory, 1617 Cole Blvd., Golden, CO 80401

Annual Battery Conference: Advances and Applications
Long Beach, California
January 9-12, 2001

ABSTRACT

Battery management is essential for achieving desired performance and life cycle from a particular battery pack in Electric and Hybrid Vehicles (EV and HEV). The batteries must be thermally managed in addition to the electrical control. In order to design battery pack management systems, the designers need to know the thermal characteristics of modules and batteries. Thermal characteristics that are needed include heat capacity of modules, temperature distribution and heat generation from modules under various charge/discharge profiles. In the last few years, we have been investigating thermal management of batteries and conducting tests to obtain thermal characteristics of various EV and HEV batteries. We used a calorimeter to measure heat capacity and heat generation from batteries and infrared equipment to obtain thermal images of battery modules under load. In this paper, we will present our approach for thermal characterization of batteries (heat generation, heat capacity, and thermal images) by providing selected data on valve regulated lead acid, lithium ion, and nickel zinc battery modules/cells. For each battery type, the heat generation rate depends on the initial state of charge, initial temperature, and charge/discharge profile. Thermal imaging indicated that the temperature distribution in modules/cells depends on their design.

Introduction

Electric and hybrid electric vehicles are under development or production today by various manufacturers as one way to improve fuel economy and reduce emission to meet various local, national, and global challenges. The performance and life-cycle costs of electric vehicles (EVs) and hybrid electric vehicles (HEVs) depend inherently on their energy storage systems such as batteries. Battery pack performance directly affects the all-electric range, power for acceleration, charge acceptance during energy recovery from regenerative braking, fuel economy, and emissions. Because the battery pack cost, durability, and life cycle also affect the cost and reliability of the vehicle, any parameter that affects the battery pack must be optimized.

Temperature range and uniformity in a pack are important factors for obtaining optimum performance from an EV or HEV battery pack. All the modules in a pack should operate within the optimum temperature range suitable for the particular electrochemical pair used. Equally important, modules need to be operated at uniform temperatures because uneven temperature distribution in a pack leads to different charge/discharge behavior, which, in turn, leads to electrically unbalanced modules and reduced pack performance *(1)*. As part of the Partnership for New Generation Vehicles (PNGV) and the U.S. Department of Energy's (DOE) Hybrid Electric Vehicle Program *(2)*, engineers from National Renewable Energy Laboratory (NREL) have been working with U.S. automobile manufacturers and their battery pack suppliers and have developed capabilities specific to battery pack thermal management issues. These capabilities include a calorimeter to measure heat generation from batteries under cycling, heat capacity (or specific heat), thermal conductivity estimation, and module temperature distribution visualization using thermal imaging. The information is used for evaluation, analysis, and design of modules and battery packs *(3)*. We have investigated thermal characteristics and performance of various EV and HEV modules and cells with various electrochemistries such as lead acid, lithium ion, NiMH, lithium ion polymer, and nickel zinc. This paper provides a summary of our thermal characterization studies for three of these batteries.

Heat Capacity

Thermal mass (heat capacity * mass) of modules is needed for performing transient analysis of battery modules and pack to design or project how fast a pack or module cools down or heats from its initial temperature in a given surrounding. To estimate the thermal mass m_t the module, one can use the heat capacity (C_p) and mass (m) of each component/material in the module and calculate the mass - weighted average thermal mass ($m_t = \Sigma\ C_{p,i} * mi$) or use a calorimeter to measure effective heat capacity of a module. Measuring provides a better number, due to changes of heat capacity depending on initial state of charge and temperature effects.

At NREL, we have been using a state-of-the-art calorimeter (left picture in Fig. 1) to measure the heat capacity (specific heat) of various batteries. The principle for measuring heat capacity comes from the definition of heat capacity, "*amount of heat required to cool or heat 1 kg of a material by 1°C.*" In order to measure the heat capacity of a cell/module (or any sample), we place a cell, with known mass (m) equilibrated at initial temperature T_m in the test cavity of the calorimeter (right picture in Fig. 1) maintained at T_c. After a soak period, the cell temperature reaches the cavity temperature. The calorimeter, using heat flux sensors, measures the heat (Q) exchanged between the cell and the calorimeter. Therefore, knowing the mass (m) of the cell and the temperature difference (T_m-T_c), one can calculate the heat capacity with the following equation:

$$C_p = Q / m (T_m - T_c)$$

It should be noted that our calorimeter is of the heat conduction type *(4)*, and is a modified version of a commercially available isothermal calorimeter (CSC Model 4400 Isothermal Microcalorimeter). Our custom-made calorimeter is designed for measuring heat capacity and heat generation of small HEV to large EV battery modules and cells. The test chamber in calorimeter is 39 cm long, 21 cm wide, and 20 cm high. The calorimeter bath temperature operates between -30°C and +60°C, and is controlled to within 0.001°C. With enhancements we have made, the calorimeter can measure a minimum heat of 15 J (a very small quantity of heat) and a minimum heat rate of 15 mW. We also measure heat released due to self-discharge of batteries during testing to exclude it if needed *(5)*.

Fig. 1 NREL Heat Conduction Calorimeter (on the left) and its Test Chamber containing Cells (on the right)

To establish the accuracy of the calorimeter, the heat capacity of a known mass of 6061-T6 aluminum block was measured for calibration purposes. The aluminum heat capacity we measured at an average temperature of 41.7°C was 872.5 J/Kg/°C, which is within 2.6% of the literature value of 896 J/Kg/°C.

Table 1 summarizes the heat capacity of several different batteries (modules or cells) we have tested thus far, which can be released publicly. The heat capacity of each cell/module should be close to heat capacity of the major constituents contained in the battery and its case.

Table 1. Typical Heat Capacity (Specific Heat) of Selected EV and HEV Batteries

Battery	Application	Average Battery Temp (°C)	Heat Capacity (J/kg/°C)
NiMH – 20 Ah	HEV	33.2	677.4
Li Ion - 6 Ah	HEV	33.1	795
Lithium Ion Polymer – 4 Ah	EV	18	1011.8
NiMH – 90 Ah	EV	33.9	787.5
Ni MH – 6.5 Ah	HEV	32.9	521
VRLA – 16.5 Ah	HEV	32	660

Heat Generation Rate

As mentioned before, the heat generated by a particular battery is needed for proper design of a thermal management system *(3)*. It is well-known that the heat generated by a battery is due to resistive (I^2R) losses and the enthalpy changes due to electrochemical reactions during charge or discharge. Heat generation rate from a battery module depends on several factors;

- Chemistry and construction
- Initial and final state of charge
- Battery temperature
- Charge or discharge rate and profile

In order to measure the heat generation from a battery with our calorimeter, the test chamber and module must come to a desired steady state temperature before and after the module/cell is cycled. The calorimeter and the module (with desired SOC) are brought to the desired temperature either independently or while the module is in the calorimeter.

Typical conditioning charges, capacity measurements, and SOC preparation are conducted taking up to 6-10 hours, depending on the mass of the module. It may take another 8-12 hours for the module and the calorimeter cavity to come to thermal equilibrium, mostly due to large thermal mass of the calorimeter. Then, a desired load is applied to the module with battery cyclers (such as AeroVironment ABC-150 or Bitrode FTN-300-48). The cycling, such as constant current, voltage, or power charge/discharge, or any driving profile (for example FUDS, GDST, or US06) may take 10 to 120 minutes. However, the calorimeter requires another 6-10 hours for the temperature of the module and test chamber to equilibrate. The following sections provide results on various batteries at various rates and temperatures.

Optima Valve Regulated Lead Acid HEV Module

We tested an Optima HEV module (starved, spiral wound design) developed under the DOE/GM cost-shared Hybrid Vehicle Program. The 6.68 kg module is nominally rated at 16.5 Ah. We measured the heat generation of the HEV module during the Optima recommended charging scheme and for the discharge rates of C/2, C/1, 2C, and 5C. The heat generation of the module for the four different discharge rates was measured at 0°C, 25°C, and 45°C. The self-discharge rate of the module was also measured at the end of charge or discharge for the aforementioned temperatures to correct for heat rate calculations *(5)*.

The module was placed within the calorimeter and allowed to come to thermal equilibrium. The module was then charged at a C/1 rate until the voltage of the module reached 14.2 volts. The voltage limit of 14.2 volts was held until the current was below 1.5 amps. The module was then overcharged with 1.5 amps for 1 hour. Once the module and calorimeter were again in thermal equilibrium (approximately 12 hours), the module was discharged at a rate of C/2, C/1, 2C, or 5C until the module voltage was less than 10.5 Volts. There were sufficient rest periods between each charge and discharge for achieving thermal equilibrium. Heat generation was measured during discharge from 100% SOC to 0% SOC, whereas heat generation during charge was measured from 0% SOC to 100% SOC.

Figure 2 shows the calorimeter response (heat rate) for the C/1 full discharge of the module at 0°C, 25°C, and 45°C. The heat rate was integrated with respect to time in order to determine the heat generated during the cycle. The 0°C and 25°C heat rate curves are quite similar. . However, Table 2 shows that the discharge efficiency at 45°C is greater than at 0°C and 25°C. The conundrum is solved when we compare the discharge capacities - 9.29 Ah at 45°C, 7.12 Ah at 25°C, and 4.48 Ah at 0°C. A greater discharge time would naturally result in more heat being generated during the cycle but also results in a higher efficiency. It should be noted that the average heat rate over the 5C cycle at 0°C was 96.4 Watts whereas the average heat rate was 67.2 Watts at 45°C. A summary of the constant current discharge cycles and the Optima recommended charge cycles at the three temperatures is shown in Table 2.

Table 2: Optima HEV tested under the Constant Discharge and Optima Recommended Charge Scheme

Cycle	Discharge/ Charge Capacity (Ah)	Initial Temp. (°C)	Elec. Energy Output (J)	Elec. Energy Input (J)	Calorimeter Heat Generated (J)	Efficiency (%)	Average Heat Rate/Module (W)
C/2 Discharge	10.58	0	450300	-	21800	95.2	4.69
C/1 Discharge	8.47	0	363400	-	13400	96.3	7.27
2C Discharge	6.60	0	278400	-	16000	94.2	22.3
5C Discharge	4.48	0	183700	-	19100	89.6	96.4
Recommended Charging Scheme after C/1 Discharge	8.62	0	-	449400	75700	83.2	9.88
C/2 Discharge	11.71	25	504700	-	15600	96.9	3.02
C/1 Discharge	10.39	25	448600	-	17500	96.1	7.70
2C Discharge	9.01	25	384600	-	24400	93.6	24.8
5C Discharge	7.12	25	295200	-	26400	91.1	84.1
Recommended Charging Scheme after C/1 Discharge	12.30	25	-	616200	124700	79.8	14.5
C/2 Discharge	14.48	45	624200	-	10800	98.2	1.9
C/1 Discharge	13.10	45	563800	-	6900	98.8	2.4
2C Discharge	11.76	45	499800	-	14900	97.0	11.6
5C Discharge	9.29	45	384300	-	27200	92.9	67.2
Recommended Charging Scheme after C/1 Discharge	14.20	45	-	678900	87500	87.1	19.1

The average cell/module heat rate in Watts is determined by the following equation:

$$AverageCellHeatRate = \frac{HeatGenerated}{CycleTime}$$

The heat generated is in Joules and is divided by the cycle time in seconds. The cycle time is the time over which modules experience a load, for example, at a nominal C/1 discharge from 100% to 0% SOC, the cycle time is about 3600 seconds.

One can also measure the energy efficiency of the module under charge, discharge, or cycling, knowing the electrical energy input/output and heat generated from the module (which actually is due to inefficiency of the battery). The efficiency of the module during constant charge/discharge cycles was determined by the following equation:

$$Eff = [1 - (HeatGenerated / Energy(Input \ldots Output))] * 100$$

Table 2 shows the energy efficiency of each charge or discharge half-cycle for the Optima HEV VRLA battery. The heat generation rate varied between 1.9 Watts for a C/2 discharge at 45^{o}C to 96.4 Watts for a 5C discharge at 0^{o}C. The maximum efficiency of the module, 98.8%, was measured at 45^{o}C for a C/1 discharge (16.5 amps). The minimum discharge efficiency was 89.6% at 0^{o}C for a discharge rate of 5C (82.5 amps). The charge efficiency of the module was highly variable and was measured between 79.8% and 87.1%. The charge efficiency varied because of the lack of a temperature compensated charge algorithm. Using the same charge algorithm for all temperatures causes varying amounts of overcharge and therefore results in varying charge efficiencies at different temperatures.

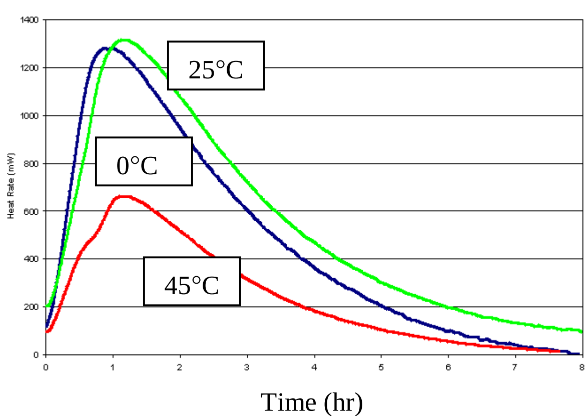

Fig. 2 Heat Rate for C/1 Full Discharge of an Optima HEV Module at various Temperatures

Evercel Nickel Zinc EVCells/Module

Recently, Evercel has introduced a Nickel Zinc (Ni-Zn) rechargeable battery for EV applications to the market. Their literature indicated that the new Ni-Zn battery performance and cycle life were close to those of NiMH, but with about 1/10th of the NiMH cost *(6).* We acquired two (1.7 V) cells and two (12 V) modules (7 cells per module) for thermal characterization. The Evercel EV cell and module are shown in Figure 3. The module/cell is nominally rated at 22 Ah at 25°C. We measured the heat generation of the EV module at various rates.

The module was charged at room temperature at a C/1.75 rate until the voltage of the module reached 14.7 Volts. Then, after a five-minute rest, a voltage limit of 14.35 Volts was held until the current was below 5.5 Amps. The module was then placed within the calorimeter and allowed to come to thermal equilibrium. Once the module and calorimeter were in thermal equilibrium (approximately 12 hours), then the module was discharged at a rate of C/2 or C/1 until the module voltage was less than 8.4 Volts. The heat generation measured during discharge was from 100% SOC to 0% SOC.

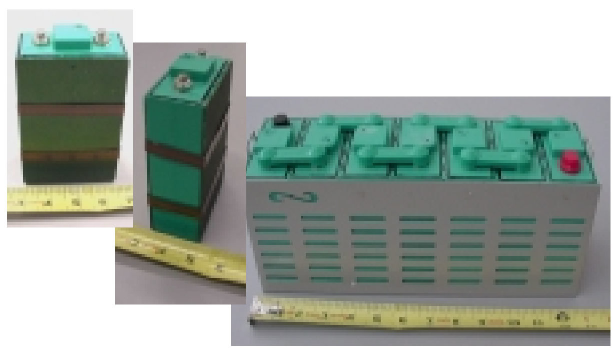

Fig. 3 Evercel Nickel Zinc Cell and Module for EV Applications

Table 3 shows results of measurements with varying discharge rates at 0^{o}C and 25^{o}C. It should be noted that the manufacturer's temperature compensated battery charging algorithm was not optimized for 0°C, since the amp-hour capacity of the battery consistently dropped during consecutive discharge cycles. Essentially, the battery was not receiving the appropriate amount of overcharge to maintain a consistent discharge capacity. We are presently working with the manufacturer to come up with an improved charging algorithm.

Table 3: Heat Generation Evercel Nickel Zinc EV Module tested under Constant Discharge

Cycle	Discharge Capacity (Ah)	Initial Temperature (^oC)	Average Heat Rate/Module (W)
C/3 Discharge	24.9	25	16.2
C/2 Discharge	24.7	25	25.7
C/1 Discharge	23.5	25	57.1
5C Discharge	23.4	25	488.4
C/2 Discharge	19.74	0	30.49
C/1 Discharge	15.57	0	74.65

Saft Lithium Ion HEV Cells

We measured the heat generation from 6 Ah high power cells from Saft. The Li-Ion cylindrical cells were spiral-wound and consisted of a plastified carbon anode, a lithiated metal oxide cathode, and an organic electrolyte *(7).* The nominal voltage of each 0.375 kg cell was 3.6 V. Heat generation from the cell was measured for both constant current charges/discharges and also under a relatively aggressive driving profile, the US06, at various initial stages of charge and temperatures (–20°, 0°, 22°, and 50°C).

At 22°C, discharging from 80% to 50% SOC, the heat generation rate was 0.13, 10.5, and 41.6 Watts for C/1, 5C, and 10C discharge rates, respectively. As the rate increased and temperature decreased, the heat generation rate increased. Figure 4 shows the heat generation from one Saft cell during the US06 driving profile at various initial temperatures and SOC.

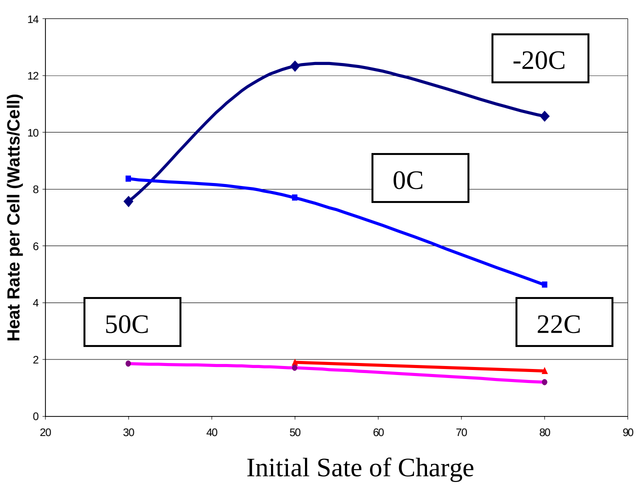

Fig 4. Heat Generated from a Lithium Ion HEV Cell

Thermal Imaging

Infrared (IR) equipment is generally used to obtain a thermal finger-print of the surface of any object. Different surface temperatures from an object radiate different energies that a camera equipped with an IR detector can capture. The IR equipment converts the energy back to temperature. This is a great tool for finding hot spots or temperature distribution on the surface of an object without using any intrusive temperature sensors. These surface temperatures are indicative of internal temperatures in the object. The IR thermal imaging could also be used as a diagnostic tool for finding problem spots in a battery.

Over the last few years, we have captured thermal images of various cells/modules to qualitatively evaluate the thermal behavior and temperature distribution in modules and also diagnose any peculiar thermal behavior.

Figure 5 shows thermal images of the Optima HEV battery at the end of the Optima recommended charging scheme and at the end of a 2C discharge. The face of the battery underneath the positive terminal is imaged, as well as the side underneath the negative terminal. The module shows localized heating in the face and side images during the charging profile. The location of the heating indicates that the cast on strap (cell to cell interconnects) may not be wetting well with the foil sheets or may not be optimized for the high currents. The discharge thermal images show localized heating at the center cell and where the cells meet one another. The higher temperature in these areas is indicative of the smaller surface area that is exposed to ambient air.

Figure 6 shows thermal image of three Saft 6 Ah Lithium ion cells without any air-cooling after eight US06 driving cycles (80 minutes). The temperature distribution in each cell is uniform due to the high thermal conductivity of the casing material.

Figure 7 shows the thermal image of the Evercel Ni-Zn cell at the end of the C/1 discharge. It can be seen that the temperature profile across the battery is quite symmetrical and the temperature variation on the cell are not large. No localized heating was seen this early in cycle life.

Concluding Remarks

This paper discussed three techniques we used for thermal characterization of batteries. We use a calorimeter to measure heat capacity and heat generation from batteries and infrared equipment to obtain thermal images of battery modules under load. The results of heat generation, heat capacity, and thermal imaging on selected valve regulated lead acid, lithium ion, and nickel zinc battery modules/cells were discussed. For each battery type, the heat generation rate depends on the initial state of charge, initial temperature, and charge/discharge profile. Thermal imaging indicated that the temperature distribution in modules/cells depend on their design. Such battery thermal characterizations can facilitate designing more robust battery thermal management systems for EVs and HEVs.

Acknowledgments

The authors would like to express their appreciation to Mark Mihalic of NREL, who performed most of the experiments discussed here. This work was funded by U.S. Department of Energy, Office of Advanced Automotive Technologies (Bob Kost, Program Manager). We appreciate our battery partners for providing batteries and technical insight.

References

1. Pesaran, A.A., Vlahinos, A., Burch, S.D., "Thermal Performance of EV and HEV Battery Modules and Packs," *Proceedings of the 14th International Electric Vehicle Symposium*, Orlando, Florida, December 15–17, **1997**.
2. Oswald, L.J. and Skellenger, G.D. "The GM/DOE Hybrid Vehicle Propulsion Systems Program: A Status Report," *Proceedings of the 14th International Electric Vehicle Symposium*, Orlando, Florida, December 15–17, **1997**.
3. Pesaran, A.A., Burch, S. and Keyser, M., "An Approach for Designing Thermal Management Systems for Electric and Hybrid Vehicle Battery Packs," *Proceedings of the 4th Vehicle Thermal Management Systems*, London, UK, May 24-27, **1999**.
4. Pesaran, A.A., Russell, D.J., Crawford, J.W., Rehn, R., and. Lewis, E.A., "A Unique Calorimeter-Cycler for Evaluating High-Power Battery Modules," *Proceedings of the 13th Annual Battery Conference: Applications and Advances*, Long Beach, California, January 13–16, **1998**.
5. Keyser, M., Pesaran, A.A., Mihalic, A., and Zolot, M, " Thermal Characterization of Advanced Battery Technologies for EV and HEV Applications," *NREL Report*, August **2000**.
6. Coates, D., Rotondo, J., and Charkey A., "Nickel Zinc: A New/Old Technology," *Electric & Hybrid Vehicle Technology International Magazine*, UK & International Press, Dorking, United Kingdom (ISSN 1362-5217), **1999,** pp.124-127.
7. Chagnon, G., Oweis, S., and Sack, T., "High Power Lithium-Ion Batteries," *Proceedings of the 15th International Electric Vehicle Symposium*, Brussels, Belgium, October 1–October 3, **1998**.

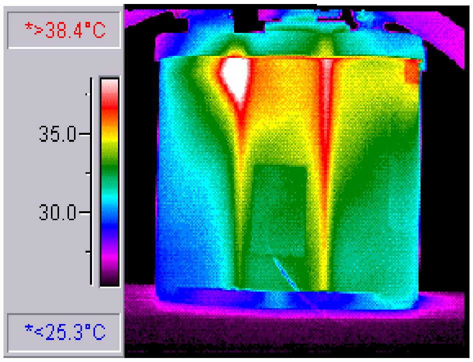

a) Face at end of charge.

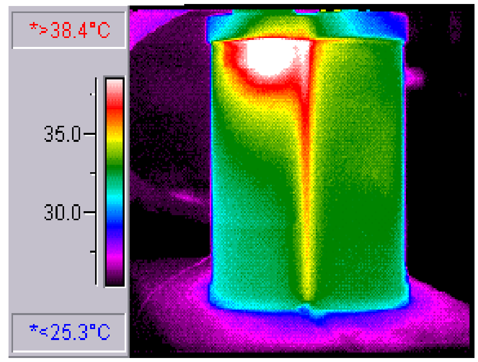

b) Side at end of charge.

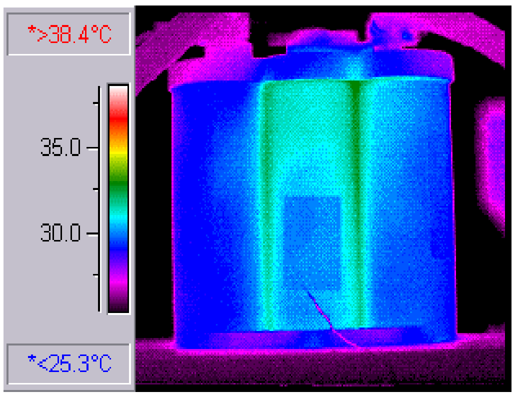

c) Face at end of 2C discharge.

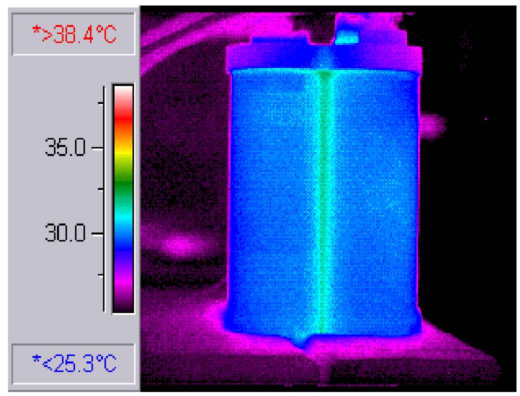

d) Side at end of 2C discharge.

Fig. 5 Thermal Images of an Optima HEV Module and Manufacturer's Specified Charge and 2C Discharge

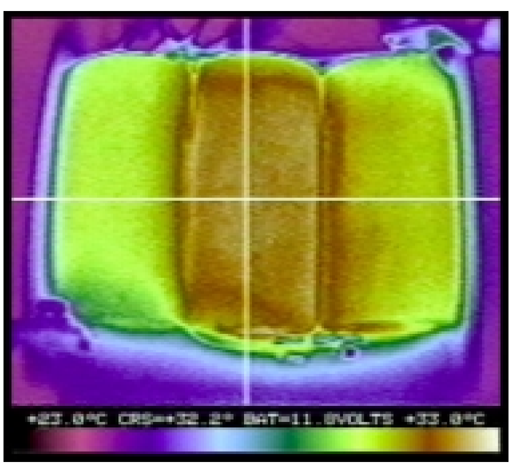

Fig. 6 Thermal Images of Three Saft HEV Lithium Ion Cells after Eight US06 Driving Profile

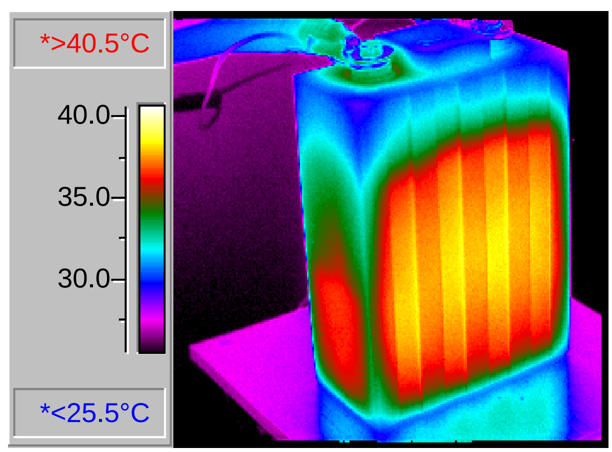

Fig. 7 Thermal Images of a Evercel Nickel Zinc Cell at the end of C/1 Discharge